

# On the Use of Adaptive Mesh Refinement for Modelling the Taylor Impact Test with the CEL Formulation

François Ducobu<sup>1,a\*</sup>, Olivier Pantalé<sup>2,b</sup>,  
Laurent Spitaels<sup>1,c</sup> and Domenico Umbrello<sup>3,d</sup>

<sup>1</sup>Machine Design and Production Engineering Lab, Research Institute for Science and Material Engineering, University of Mons, Mons, Belgium

<sup>2</sup>Université de Toulouse, UTTOP, LGP, Tarbes, France

<sup>3</sup>Department of Mechanical, Energy and Management Engineering, University of Calabria, Arcavacata, CS, Italy

<sup>a</sup>Francois.Ducobu@umons.ac.be, <sup>b</sup>Olivier.Pantale@uttop.fr,  
<sup>c</sup>Laurent.Spitaels@umons.ac.be, <sup>d</sup>domenico.umbrello@unical.it

**Keywords:** Taylor impact test, finite element, CEL, adaptive mesh refinement, Johnson-Cook.

**Abstract.** This paper examines the use of adaptive mesh refinement in Coupled Eulerian-Lagrangian (CEL) finite element modeling of the Taylor impact test. Traditional Lagrangian models suffer from severe mesh distortion under large strains, while CEL avoids this issue but requires much longer computation times. Using Abaqus/Explicit 2025, a mesh convergence study was performed to identify an accurate reference mesh. Adaptive mesh refinement was then applied to refine the mesh dynamically based on equivalent plastic strain. Results show that CEL models achieve convergence, unlike Lagrangian models, and that adaptive mesh refinement reduces computation time by up to 67%, with minimal impact on accuracy. This approach provides an efficient and reliable solution for high-strain simulations.

## Introduction

Identifying parameters of material constitutive models for modeling cutting operations is a challenging task due to the values of strain, strain rate and temperature seen by the workpiece material during that operation [1]. For a given empirical constitutive model, such as the Johnson-Cook (JC) model [2], the identification process can be performed in mainly two ways [3]: from dedicated material testing equipment results such as those used in this study, or directly from cutting experiments or simulations such as in Ducobu et al. [4] or in Klippel et al. [5].

The most used dedicated equipment for material behavior identification in these severe conditions are the Split Hopkinson Pressure Bars [6] and the Taylor impact test [7]. Inverse identification is then carried out by comparing the experimental geometry of the specimen after deformation with the geometry from the numerical modelling of the test. The parameters of the material constitutive behavior are adjusted in the model for the numerical and experimental geometries to match.

The Lagrangian formulation has long been the natural choice for modeling this type of test [8]. The mesh and the material being tied together, however, often leads to strong mesh deformations due to the large strains. This leads to a decrease in the quality of the results, and consequently of the identification procedure and of the value of the material parameters. The Coupled Eulerian-Lagrangian (CEL) formulation avoids these issues because the mesh is no longer tied to the material. It has already been successfully applied in the modeling of cutting operations [9]. Although it suppresses the problem of elements distortion, the computation times are usually significantly higher than for a model using the Lagrangian formulation, mainly due to a higher number of elements.

This study introduces the adaptive mesh refinement technique in the CEL modeling with the main objective of reducing the computation time without degrading the quality of the results. The CEL formulation has already been adopted for the 3D coupled stress-heat transfer modelling of the Taylor impact [10]; the current implementation of the adaptive mesh refinement is limited to adiabatic analysis. The main contributions of this paper by comparison to Ducobu et al. [10] are the introduction

of the adaptive mesh refinement in the CEL formulation, the study of the influence of the mesh size on the quality of the results and the CPU computation time, as well as the reduction of the computation without degradation of the results.

The paper starts by comparing the Lagrangian and CEL models in adiabatic conditions and by determining the best mesh to be used through a mesh convergence study. The adaptive mesh refinement technique is then introduced and the results are compared to the previous CEL models.

### Presentation of the finite element models

A Lagrangian model and a CEL model are developed in the frame of this study. They are 3D finite element models using Abaqus/Explicit 2025 with the same conditions as Ming and Pantalé [11] and Ducobu et al. [10]. A quarter of the actual configuration is modelled with adequate boundary conditions to reduce computation time. The specimen is a cylinder of 32.4 mm long and 3.2 mm radius. Initial conditions are a speed in the axial direction of 200 m/s and a specimen temperature of 293 K. The simulation is run for 80  $\mu$ s. Contact conditions between the specimen and the rigid plate are assumed to be perfect without friction.

The Lagrangian model includes only the specimen, while the CEL model must include the volume where the specimen will deform. This results in a larger mesh for CEL. To reduce computation time as much as possible, the initial void where the specimen will deform has a conical shape and the volume surrounding the initial cylinder is also meshed, as shown in Fig. 1. The mesh of the specimen is the same for both models. It must be noted that the size of the model and the boundary conditions were selected to avoid any loss or gain of mass during the simulations.

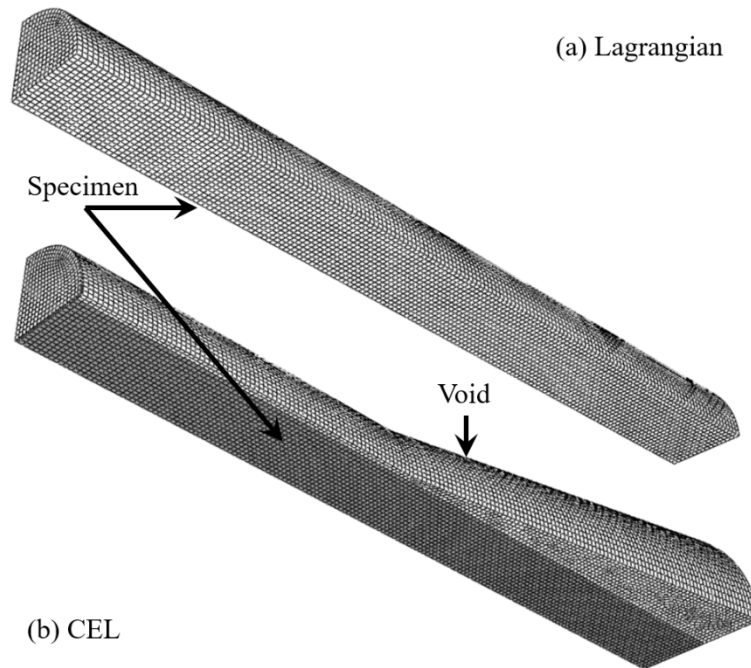


**Fig. 1.** Initial geometry and fine mesh of the Lagrangian (a) and CEL (b) models

The behavior of the specimen is modeled with JC constitutive model [2]:

$$\sigma_{JC} = [A + B \cdot \varepsilon^n] \cdot \left[ 1 + C \cdot \ln \left( \frac{\dot{\varepsilon}}{\dot{\varepsilon}_0} \right) \right] \cdot \left[ 1 - \left( \frac{T - T_{\text{room}}}{T_{\text{melt}} - T_{\text{room}}} \right)^m \right]. \quad (1)$$

Five constants need to be identified:  $A$ ,  $B$ ,  $n$ ,  $C$  and  $m$ .  $\dot{\varepsilon}_0$  is the reference strain rate.  $T_{\text{room}}$  is the room or reference temperature and  $T_{\text{melt}}$  is the melting temperature. The specimen material is 42CrMo4-FP steel. Table 1 provides the material properties and JC parameters.

**Table 1.** Johnson-Cook parameters and material properties of 42CrMo4-FP steel [11]

$A$ [MPa]	$B$ [MPa]	$C$	$n$	$m$	$\dot{\epsilon}_0$ [s <sup>-1</sup> ]	$T_{\text{room}}$ [K]
504	370	0.025	0.17	0.793	0.01	293
$T_{\text{melt}}$ [K]	$E$ [GPa]	$\nu$	$\rho$ [kg/m <sup>3</sup> ]	$\lambda$ [W/mK]	$c_p$ [J/kgK]	$\alpha$ [K <sup>-1</sup> ]
1813	206.9	0.29	7830	34	460	$1.23 \times 10^{-6}$

The current implementation of adaptive mesh refinement in Abaqus/Explicit 2025 is limited to adiabatic analysis [12], preventing carrying out a coupled stress-heat transfer analysis. Adiabatic heating effects are, however, included due to inelastic deformation (with an inelastic heat fraction of 0.9). The element type used is 3D linear 8-node with reduced integration, meaning C3D8R elements for the Lagrangian model and EC3D8R elements for the CEL model. Computations were performed with Abaqus/Explicit 2025 on Windows 11 64 bits and 32 GB of RAM, using 4 cores of an Intel i9-13900HX @ 1.70-5.40 GHz processor and double precision.

### Influence of Mesh Size on the Results

A mesh sensitivity analysis on the results of both Lagrangian and CEL models is performed to assess the influence of the mesh size on the results and determine the best mesh size to use for the simulation of the 3D Taylor impact test. The Lagrangian model is the reference as this formulation is well-known and widely adopted. Structured mesh is adopted (except in the conical region of the CEL model) with 4 different element sizes: coarse (mean element size of 0.8 mm), medium (mean element size of 0.4 mm), fine (mean element size of 0.2 mm) and very fine (mean element size of 0.15 mm).

The shape of the deformed specimen can be assessed in Fig. 2 and Fig. 3. It is similar to experimental results for the same material but different specimen dimensions and speed [8]. As already observed [10], small defects, similar to indentations are noted for coarse and (slightly) medium CEL meshes mainly due to the errors in tracking the shape of the specimen in the thin void layer around the specimen. This should be reduced with an increase of the size of the void region surrounding the undeformed part of the specimen. However, as they are far from the region of interest, they do not influence the results and this would lead to an increase in computation time without benefit for the quality of the results. A similar observation is performed on the upper corner of the specimen that is rounded (or chamfered) due to the interpolation carried out by Abaqus to determine where material is. Such a rounding is inherent to the implementation of the CEL formulation and it is also noticed when it is used for other applications [9].

Table 2 provides a quantitative comparison of the results:

- $L_f$ : final length and  $R_f$ : final radius of the specimen, measured in a lateral face of the specimen.
- $\bar{\epsilon}_{\text{max}}$ : maximal equivalent plastic strain,  $\sigma_{\text{max}}$ : maximal equivalent von Mises stress and  $T_{\text{max}}$ : maximal temperature.
- $N_{\text{elements}}$ : number of elements of the model and  $\hat{t}_{\text{CPU}}$ : computation time normalized by the computation time of the Lagrangian model with a coarse mesh.

Refining the mesh globally leads to a convergence of the dimensions of the specimen for both Lagrangian and CEL models. The general trends are a reduction of the final length and an increase of the final radius of the specimen when the mesh density increases. When comparing the results of the fine and of the very fine meshes, it turns out that the fine CEL mesh is the converged case.

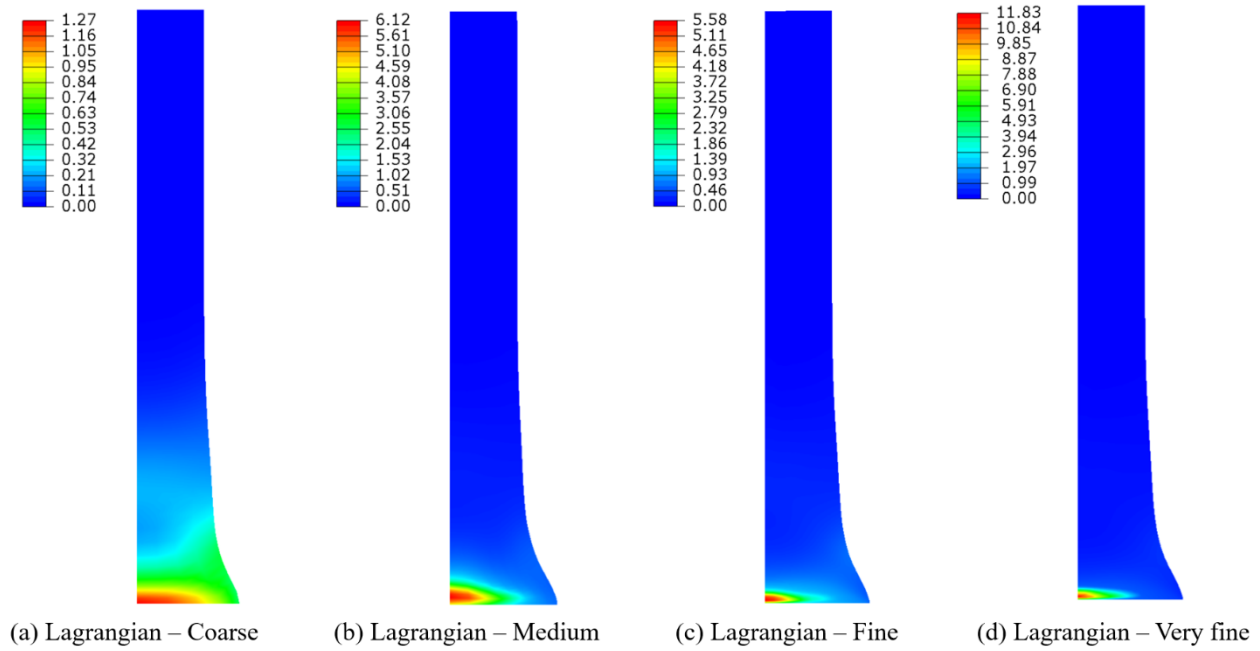


**Fig. 2.** Equivalent plastic strains for the Lagrangian coarse (a), medium (b), fine (c) and very fine (d) meshes

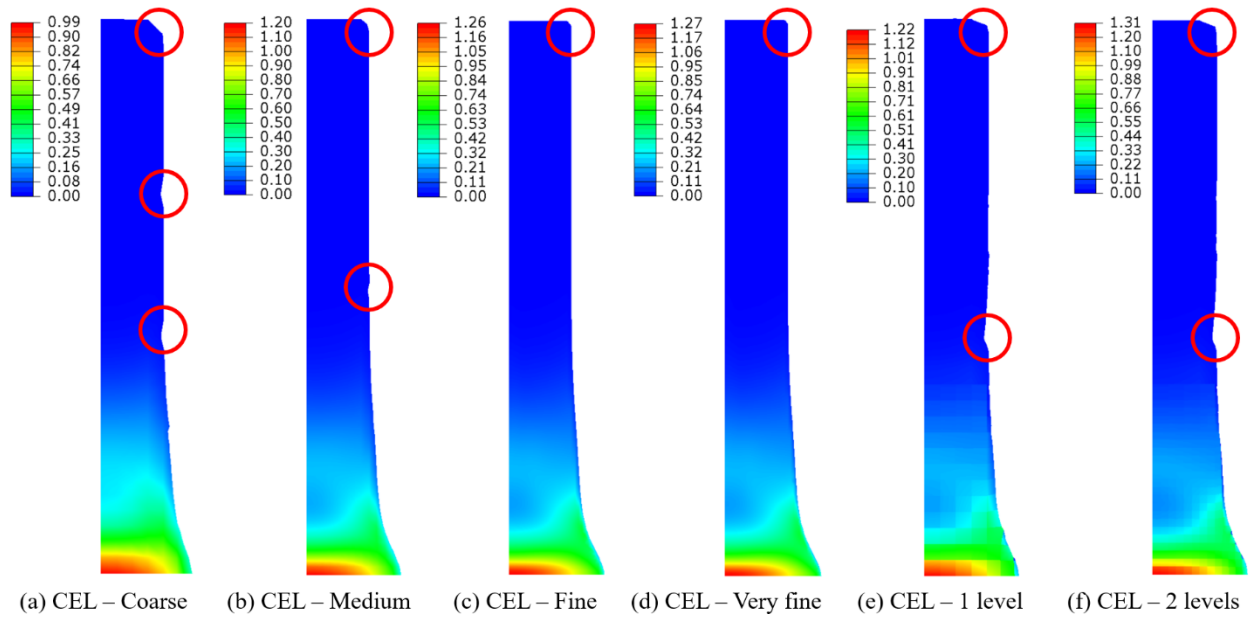


**Fig. 3.** Equivalent plastic strains for the CEL coarse (a), medium (b), fine (c) and very fine (d) meshes, and adaptive mesh refinement with 1 level (e) and 2 levels (f) meshes (rounding and indentation artifacts highlighted)

The contours (Fig. 2 and Fig. 3) of the equivalent plastic strains,  $\bar{\epsilon}$ , and the values (Table 2) of the maximal equivalent plastic strain,  $\bar{\epsilon}_{\max}$ , clearly show the mesh dependence and localization of the deformation for the Lagrangian model. As highlighted in Fig. 4, convergence is not reached, and unrealistically high and increasing values of strain are observed with denser mesh. This clearly shows that elements in the impact region of the specimen are too much deformed (Fig. 5) and that such results cannot be used. Consequently, comparing the dimensions of the specimen for both formulations, it is not surprising that the final radius is larger for the Lagrangian formulation than for the CEL formulation.

**Table 2.** Results for the different meshes with the Lagrangian and CEL formulations (converged results in bold)

Model	Coarse	Medium	Fine	Very fine
Lagrangian models				
$L_f$ [mm]	39.17	38.85	39.01	39.09
$R_f$ [mm]	6.74	7.03	6.93	6.93
$\bar{\epsilon}_{\max}$	1.27	6.12	5.58	11.83
$\sigma_{\max}$ [MPa]	678	763	913	747
$T_{\max}$ [K]	599	1357	1305	1675
$N_{\text{elements}}$	600	4860	38 880	91 800
$\hat{t}_{\text{CPU}}$	1	2	108	491
CEL models				
$L_f$ [mm]	39.08	39.07	<b>38.92</b>	39.01
$R_f$ [mm]	6.50	6.67	<b>6.74</b>	6.79
$\bar{\epsilon}_{\max}$	0.99	1.20	<b>1.26</b>	1.27
$\sigma_{\max}$ [MPa]	531	614	<b>634</b>	633
$T_{\max}$ [K]	534	583	<b>598</b>	600
$N_{\text{elements}}$	1080	8477	<b>67 340</b>	150 998
$\hat{t}_{\text{CPU}}$	3	15	<b>412</b>	1334

The maximal equivalent von Mises stress,  $\sigma_{\max}$ , and the maximal temperature,  $T_{\max}$ , values globally follow the same trend as expected. The absence of mesh deformation for the CEL formulation prevents these localizations and allows to reach convergence. The results of the CEL model are therefore more accurate and reliable.

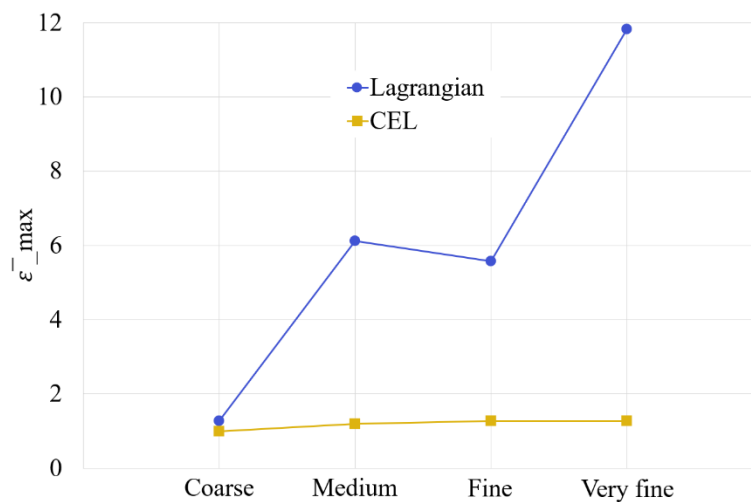


**Fig. 4.** Illustration of the convergence of the maximal equivalent plastic strain for the CEL formulation and not for the Lagrangian formulation

As expected, refining the mesh increases the computation time whatever the formulation. The computation time is larger for the CEL formulation due to a higher number of elements for the same mesh density. The better accuracy and reliability of the CEL model have therefore a CPU cost.

### Introduction and influence of adaptive mesh refinement for the CEL formulation

**Presentation of adaptive mesh refinement in CEL.** Now that the mesh size to use for the 3D simulation of the Taylor impact test is determined, adaptive mesh refinement is considered to reduce the computation time of the CEL formulation (i.e. its disadvantage by comparison to the Lagrangian

formulation) without degrading the quality of the results. The ultimate goal would be to obtain results as accurate as with the fine mesh for computation times as low as those with coarse meshes.

The adaptive mesh refinement allows to refine the mesh in the 3 directions of space by the same factor for each element satisfying a defined criterion [12]. One level of refinement consists of dividing 1 element into 8 elements (i.e. each side of the initial element is divided by 2). The number of levels is in theory not limited, but preliminary tests showed that a level higher than 2 was leading to the immediate termination of the computation. However, this limitation does not impact the current study as 2 levels is what is needed. Indeed, dividing the edges of the elements from the coarse mesh (0.8 mm) in 4 gives the same mesh size as the fine converged mesh (0.2 mm).

Adaptive mesh refinement is applied to the CEL model with coarse mesh with a value of 0.1 for the equivalent plastic strain,  $\bar{\epsilon}$ , as refinement criterion (this value has been set following a preliminary sensitivity study). It means that any element with a  $\bar{\epsilon}$  value of 0.1 will be divided into 8 elements for 1 level of refinement and into 64 elements for 2 levels of refinement. The minimum element size with 1 level of mesh refinement corresponds to the elements size of the medium mesh, while it is to the fine mesh for 2 levels of mesh refinement.

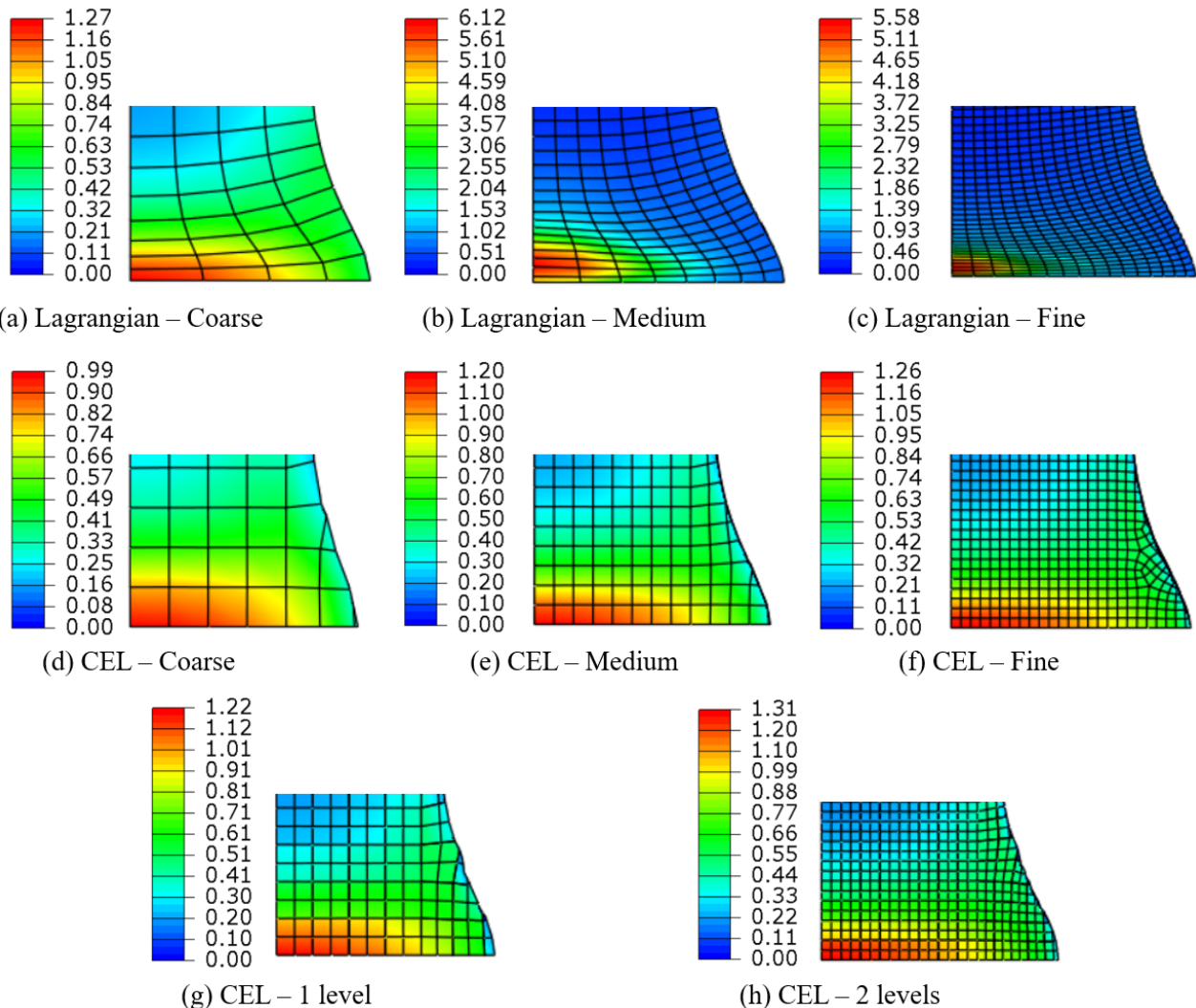


**Fig. 5.** End of the deformed specimen results showing the mesh and the equivalent plastic strains for the Lagrangian coarse (a), Lagrangian medium (b), Lagrangian fine (c), CEL coarse (d), CEL medium (e), CEL fine (f), and CEL adaptive mesh refinement with 1 level (g) and 2 levels (h) meshes

**Results and discussions.** Fig. 3 shows the deformed specimens at the end of the simulation, while Fig. 5 demonstrates the refinement of the mesh in the areas where  $\bar{\epsilon}$  is larger than 0.1. The results are qualitatively close to those without adaptive mesh refinement. The quantitative comparison using

values from Table 3 confirms that the dimensions of the deformed specimen are close with and without adaptive mesh refinement. Differences between the medium mesh and 1 level of refinement are close to 2%, while they are close to 1% between the fine mesh and 2 levels of refinement. Similarly, the maximal equivalent plastic strain, the maximal equivalent von Mises stress, and the maximal temperature are close.

The dramatic change is to be found in the computation time. Indeed, reductions of 27% and 67% are observed when using adaptive mesh refinement by comparison to the medium and fine meshes, respectively. The objective when introducing adaptive mesh refinement in the CEL models is therefore achieved: the computation time is significantly reduced without significantly decreasing the quality of the results.

**Table 3.** Results for the CEL formulation with and without adaptive mesh refinement (results without adaptive mesh refinement are the same as in Table 2, they are included here for an easier comparison)

Model	$L_f$ [mm]	$R_f$ [mm]	$\bar{\epsilon}_{\max}$	$\sigma_{\max}$ [MPa]	$T_{\max}$ [K]	$N_{\text{elements}}$	$\hat{t}_{\text{CPU}}$
CEL Coarse	39.08	6.50	0.99	531	534	1080	3
CEL Medium	39.07	6.67	1.20	614	583	8477	15
CEL Fine	38.92	6.74	1.26	634	598	67 340	412
CEL 1 level	38.23	6.53	1.22	590	588	9720	11
CEL 2 levels	38.59	6.67	1.32	664	609	70 200	135

## Conclusions

The Taylor impact test has been modeled in 3D with Abaqus/Explicit using both Lagrangian and CEL formulations. While severe mesh distortions and localizations have been highlighted for the Lagrangian model, the CEL formulation showed better performance thanks to the absence of mesh deformation. This allowed to reach convergence of dimensions, and strains, stresses and temperatures with the CEL formulation, contrary to the Lagrangian formulation. The longer computation times for the CEL models were successfully decreased with the introduction of adaptive mesh refinement. This positive impact on computation resources did not degrade significantly (difference of max. 2%) the quality of the results. This study showed that high quality results can be obtained with the CEL formulation and for a small computation cost (reduction of CPU time up to 67%) if adaptive mesh refinement is used. Future works could expand CEL adaptive mesh refinement to other applications, and especially to cutting operations, provided it is implemented for stress-heat transfer coupled analysis.

## Acknowledgements

This research was funded by the European Union and the Walloon regional government (HybridAM research project).

## References

- [1] P.J. Arrazola, T. Özel, D. Umbrello, M. Davies, I.S. Jawahir, Recent advances in modelling of metal machining processes, *CIRP Annals* 62 (2013) 695–718. <https://doi.org/10.1016/j.cirp.2013.05.006>.
- [2] G.R. Johnson, W.H. Cook, A constitutive model and data for metals subjected to large strains, high strain rates and high temperatures, in: *Proc. 7th International Symposium on Ballistics*, The Hague, The Netherlands, 1983: pp. 541–547.
- [3] S.N. Melkote, W. Grzesik, J. Outeiro, J. Rech, V. Schulze, H. Attia, P.-J. Arrazola, R. M'Saoubi, C. Saldana, Advances in material and friction data for modelling of metal machining, *CIRP Annals* 66 (2017) 731–754. <https://doi.org/10.1016/j.cirp.2017.05.002>.

- 
- [4] F. Ducobu, N. Kugalur-Palanisamy, G. Briffoteaux, M. Gobert, D. Tuytens, P.J. Arrazola, E. Rivière-Lorphèvre, Identification of the Constitutive and Friction Models Parameters via a Multi-Objective Surrogate-Assisted Algorithm for the Modeling of Machining—Application to Arbitrary Lagrangian Eulerian Orthogonal Cutting of Ti6Al4V, *J. Manuf. Sci. Eng* 146 (2024). <https://doi.org/10.1115/1.4065223>.
- [5] H. Klippel, M. Röthlin, M. Afrasiabi, M. Kuffa, K. Wegener, Inverse identification of Johnson–Cook flow stress parameters for Ti6Al4V, *CIRP Journal of Manufacturing Science and Technology* 64 (2026) 15–31. <https://doi.org/10.1016/j.cirpj.2025.11.012>.
- [6] H. Kolsky, An Investigation of the Mechanical Properties of Materials at very High Rates of Loading, *Proc. Phys. Soc. B* 62 (1949) 676. <https://doi.org/10.1088/0370-1301/62/11/302>.
- [7] G.I. Taylor, The testing of materials at high rates of loading, *Journal of the Institution of Civil Engineers* 26 (1946) 486–519. <https://doi.org/10.1680/ijoti.1946.13699>.
- [8] I. Nistor, O. Pantalé, S. Caperaa, C. Sattouf, Identification of a dynamic viscoplastic flow law using a combined Levenberg-Marquardt and Monte-Carlo algorithm, in: VII International Conference on Computational Plasticity, COMPLAS 2003, CIMNE, Barcelona, 2003.
- [9] F. Ducobu, E. Rivière-Lorphèvre, E. Filippi, Finite element modelling of 3D orthogonal cutting experimental tests with the Coupled Eulerian-Lagrangian (CEL) formulation, *Finite Elements in Analysis and Design* 134 (2017) 27–40. <https://doi.org/10.1016/j.finel.2017.05.010>.
- [10] F. Ducobu, A. Demarbaix, O. Pantalé, Finite element modelling of the Taylor impact test in 3D with the Coupled Eulerian-Lagrangian method, in: 24th International Conference on Material Forming (ESAFORM 2021), Liège, Belgium, 2021. <https://popups.uliege.be/esaform21/index.php?id=316>.
- [11] L. Ming, O. Pantalé, An efficient and robust VUMAT implementation of elastoplastic constitutive laws in Abaqus/Explicit finite element code, *Mechanics & Industry* 19 (2018) 308. <https://doi.org/10.1051/meca/2018021>.
- [12] SIMULIA, Abaqus Documentation, Dassault Systems, 2025.